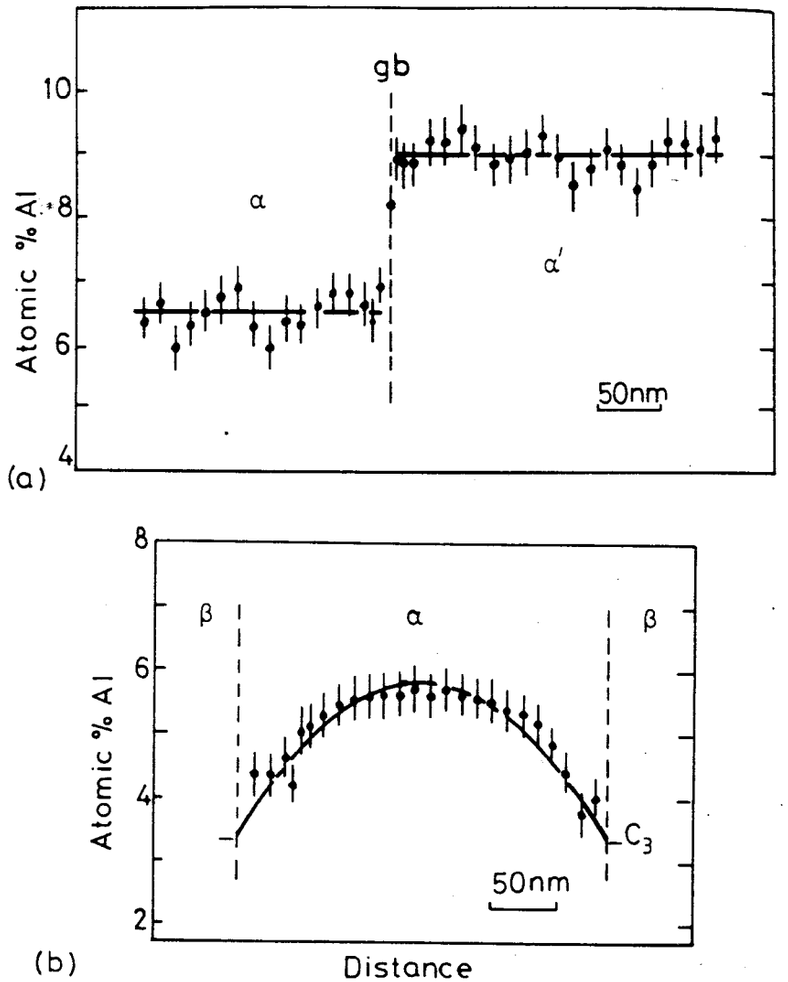

Fig. 5.54 (a) The variation of aluminium concentration across an advancing grain boundary midway between two precipitate lamellae. (b) A similar profile along a line such as S in Fig. 5.53.

nucleation by forming with an orientation relationship to one of the austenite grains, γ_1 in Fig. 5.57a. (The crystal structure of cementite is orthorhombic and the orientation relationship is close to $(100)_c//(1\bar{1}1)_\gamma$, $(010)_c//(110)_\gamma$, $(001)_c//(\bar{1}12)_\gamma$.) Therefore the nucleus will have a semicoherent, low-mobility interface with γ_1 and an incoherent mobile interface with γ_2. The austenite surrounding this nucleus will become depleted of carbon which will increase the driving force for the precipitation of ferrite, and a ferrite nucleus forms adjacent to the cementite nucleus also with an orientation relationship to γ_1 (the Kurdjumov–Sachs relationship). This process can be repeated

Fig. 5.55 A pearlite colony advancing into an austenite grain. (After L.S. Darken and R.M. Fisher in *Decomposition of Austenite by Diffusional Processes*, V.F. Zackay and H.I. Aaronson (Eds.), by permission of The Metallurgical Society of AIME.

cleation of both phases the colony can grow edgewise by the movement of the *incoherent* interfaces, that is pearlite grows into the austenite grain with which it does not have an orientation relationship. The carbon rejected from the growing ferrite diffuses through the austenite to in front of the cementite, as with eutectic solidification.

If the alloy composition does not perfectly correspond to the eutectoid composition the grain boundaries may already be covered with a proeutectoid ferrite or cementite phase. If, for example, the grain boundary already contains a layer of cementite, the first ferrite nucleus will form with an orientation relationship to this cementite on the mobile incoherent side of the allotriomorphs as shown in Fig. 5.57b. Again due to the higher mobility of the incoherent interfaces the pearlite will grow into the austenite with which there is no orientation relationship.

Whatever the pearlite nucleation mechanism, new cementite lamellae are able to form by the branching of a single lamella into two new lamellae as shown in Fig. 5.57a(iv) or c. The resultant pearlite colony is effectively two interpenetrating single crystals.

It can be seen that the nucleation of pearlite requires the establishment of cooperative growth of the two phases. It takes time for this cooperation to be established and the rate of colony nucleation therefore increases with time. In

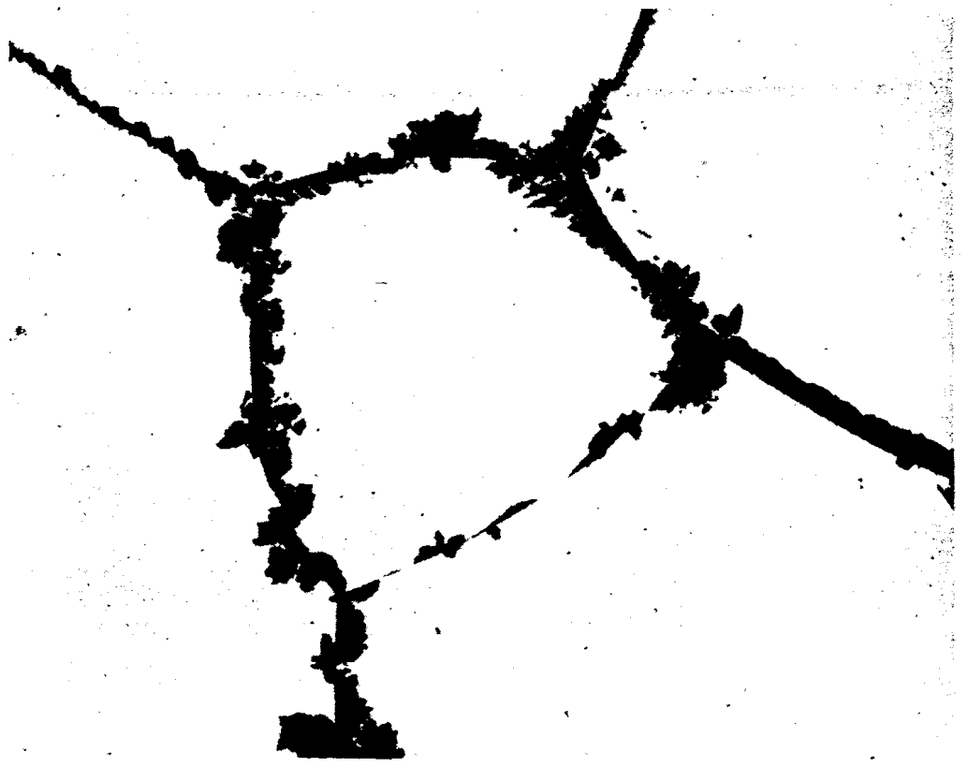

Fig. 5.56 A partially transformed eutectoid steel. Pearlite has nucleated on grain boundaries and inclusions (× 100). (After J.W. Cahn and W.C. Hagel in *Decomposition of Austenite by Diffusional Processes*, V.F. Zackay and H.I. Aaronson (Eds.), 1962, by permission of The Metallurgical Society of AIME.)

some cases cooperation is not established and the ferrite and cementite grow in a non-lamellar manner producing so-called degenerate pearlite[14].

Pearlite Growth

The growth of pearlite in binary Fe–C alloys is analogous to the growth of a lamellar eutectic with austenite replacing the liquid. Carbon can diffuse interstitially through the austenite to the tips of the advancing cementite lamellae so that the equations developed in Section 4.3.2 should apply equally well to pearlite. Consequently the minimum possible interlamellar spacing (S^*) should vary inversely with undercooling below the eutectoid temperature (A_1), and assuming the observed spacing (S_0) is proportional to S^* gives

$$S_0 \propto S^* \propto (\Delta T)^{-1} \tag{5.53}$$

Similarly the growth rate of pearlite colonies should be constant and given by a relationship of the type

$$v = kD_c^{\gamma}(\Delta T)^2 \tag{5.54}$$

where k is a thermodynamic term which is roughly constant.

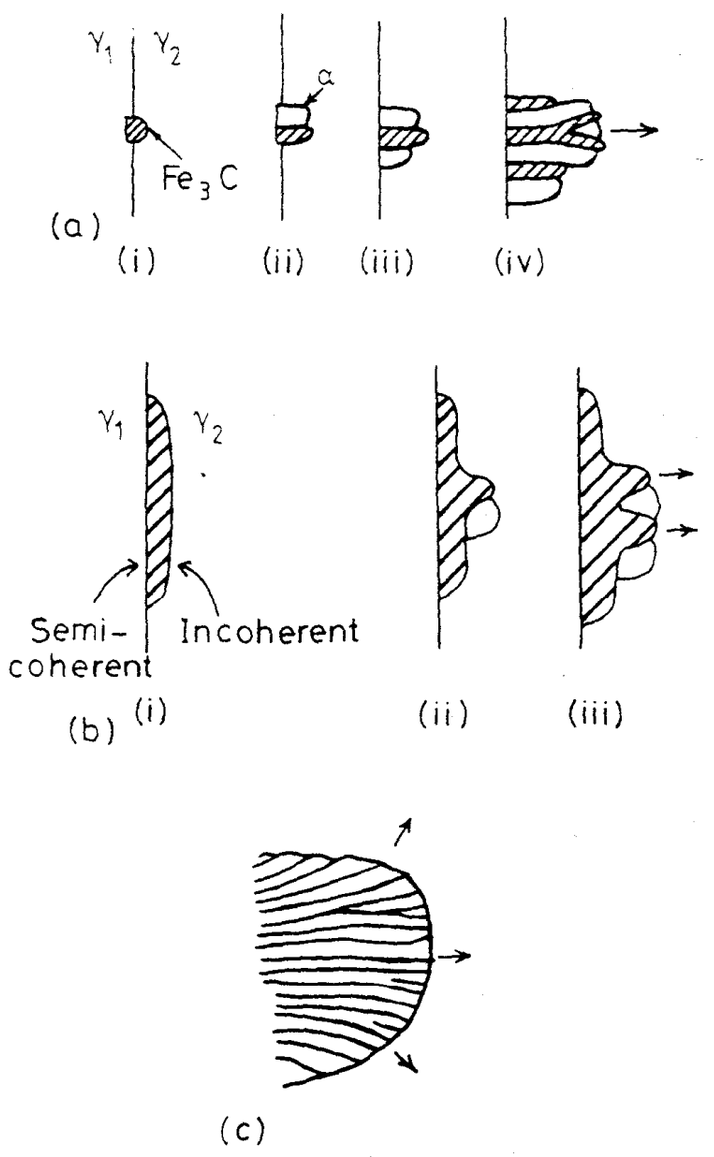

Fig. 5.57 Nucleation and growth of pearlite. (a) On a 'clean' grain boundary. (i) Cementite nucleates on grain boundary with coherent interface and orientation relationship with γ_1 and incoherent interface with γ_2. (ii) α nucleates adjacent to cementite also with a coherent interface and orientation relationship with γ_1. (This also produces an orientation relationship between the cementite and ferrite.) (iii) The nucleation process repeats sideways, while *incoherent* interfaces grow into γ_2. (iv) New plates can also form by a branching mechanism. (b) When a proeutectoid phase (cementite or ferrite) already exists on that boundary, pearlite will nucleate and grow on the incoherent side. A different orientation relationship between the cementite and ferrite results in this case. (c) A pearlite colony at a later stage of growth.

Observed spacings are found to obey Equation 5.53, varying from ~1 μm at high temperatures to ~0.1 μm at the lowest temperatures of growth[15]. However, it is found that S_0 is usually greater than $2S^*$, i.e. the observed spacing is not determined by the maximum growth rate criterion. Instead it may be determined by the need to create new cementite lamellae as the perimeter of the pearlite nodules increases. This can occur either by the nucleation of new cementite lamellae, or by the branching of existing lamellae, Fig. 5.57c.

In the case of binary Fe–C alloys, observed growth rates are found to agree rather well with the assumption that the growth velocity is controlled by the diffusion of carbon in the austenite. Figure 5.58 shows measured and calculated growth rates as a function of temperature. The calculated line is based on an equation similar to Equation 5.54 and shows that the measured growth rates are reasonably consistent with volume-diffusion control. However, it is also possible that some carbon diffusion takes place through the γ/α and γ/cementite interfaces, which could account for the fact that the predicted growth rates shown in Fig. 5.58 are consistently too low.

A schematic TTT diagram for the pearlite reaction in eutectoid Fe–C alloys is shown in Fig. 5.59. Note the 'C' shape typical of diffusional transformations that occur on cooling. The maximum rate of transformation occurs at about 550°C. At lower temperatures another type of transformation product, namely *Bainite*, can grow faster than pearlite. This transformation is dealt with in the next section.

Eutectoid transformations are found in many alloys besides Fe–C. In alloys where all elements are in substitutional solid solution, lattice diffusion is found to be too slow to account for observed growth rates. In these cases diffusion

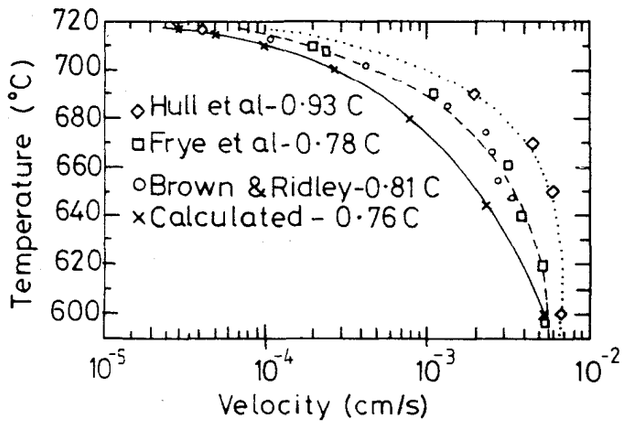

Fig. 5.58 Pearlite growth rate v. temperature for plain carbon steels. (After M.P. Puls and J.S. Kirkaldy, *Metallurgical Transactions* **3** (1972) 2777. © American Society for Metals and the Metallurgical Society of AIME, 1972.)

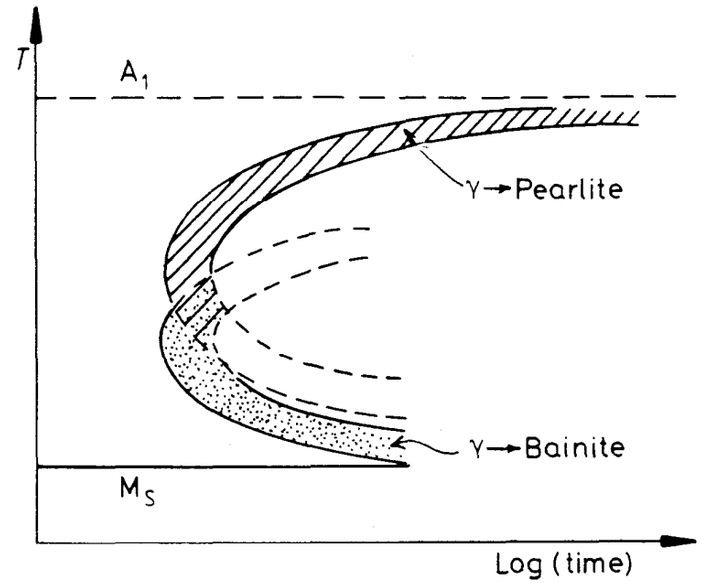

Fig. 5.59 Schematic diagram showing relative positions of the transformation curves for pearlite and bainite in plain carbon eutectoid steels.

occurs instead through the colony/matrix interface. Consideration of the diffusion problem in this case leads to a relationship of the type

$$v = kD_B(\Delta T)^3 \tag{5.55}$$

where k is a thermodynamic constant and D_B is the boundary diffusion coefficient.

Pearlite in Off-Eutectoid Fe—C Alloys

When austenite containing more or less carbon than the eutectoid composition is isothermally transformed below the A_1 temperature the formation of pearlite is usually preceded by the precipitation of proeutectoid ferrite or cementite. However, if the undercooling is large enough and the departure from the eutectoid composition is not too great it is possible for austenite of non-eutectoid composition to transform directly to pearlite. The region in which this is possible corresponds approximately to the condition that the austenite is simultaneously saturated with respect to both cementite and ferrite, i.e. the hatched region in Fig. 5.60. (See also Fig. 5.48). Thus a 0.6% C alloy, for example can be transformed to ~100% pearlite provided the temperature is low enough to bring the austenite into the hatched region of Fig. 5.60 (but not so low that bainite forms). At intermediate undercoolings some proeutectoid ferrite will form but less than predicted by the equilibrium phase diagram.

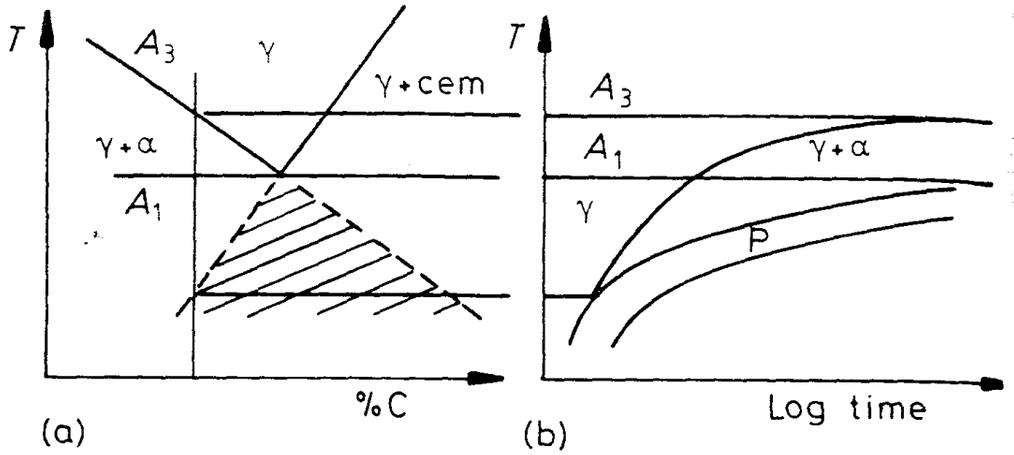

Fig. 5.60 Effect of transformation temperature on the volume fraction of proeutectoid ferrite.

Similar considerations apply to transformations during continuous cooling—larger grain sizes and faster cooling rates favour low volume fractions of ferrite. Compare Fig. 5.49c and d.

5.8.2 *The Bainite Transformation*

When austenite is cooled to large supersaturations below the nose of the pearlite transformation curve a new eutectoid product called *bainite* is produced. Like pearlite, bainite is a mixture of ferrite and carbide, but it is microstructurally quite distinct from pearlite and can be characterized by its own C curve on a TTT diagram. In plain carbon steels this curve overlaps with the pearlite curve (Fig. 5.59) so that at temperatures around 500 °C both pearlite and bainite form competitively. In some alloy steels, however, the two curves are separated as shown in Fig. 5.65.

The microstructure of bainite depends mainly on the temperature at which it forms[16].

Upper Bainite

At high temperatures (350 °C–550 °C) bainite consists of needles or laths of ferrite with cementite precipitates between the laths as shown in Fig. 5.61. This is known as *upper bainite*. Figure 5.61a shows the ferrite laths growing into partially transformed austenite. The light contrast is due to the cementite. Figure 5.61b illustrates schematically how this microstructure is thought to develop. The ferrite laths grow into the austenite in a similar way to Widmanstätten side-plates. The ferrite nucleates on a grain boundary with a Kurdjumov–Sachs orientation relationship with one of the austenite grains, γ_2, say. Since the undercooling is very large the nucleus grows most rapidly into the γ_2 grain forming ferrite laths with low energy semicoherent inter-

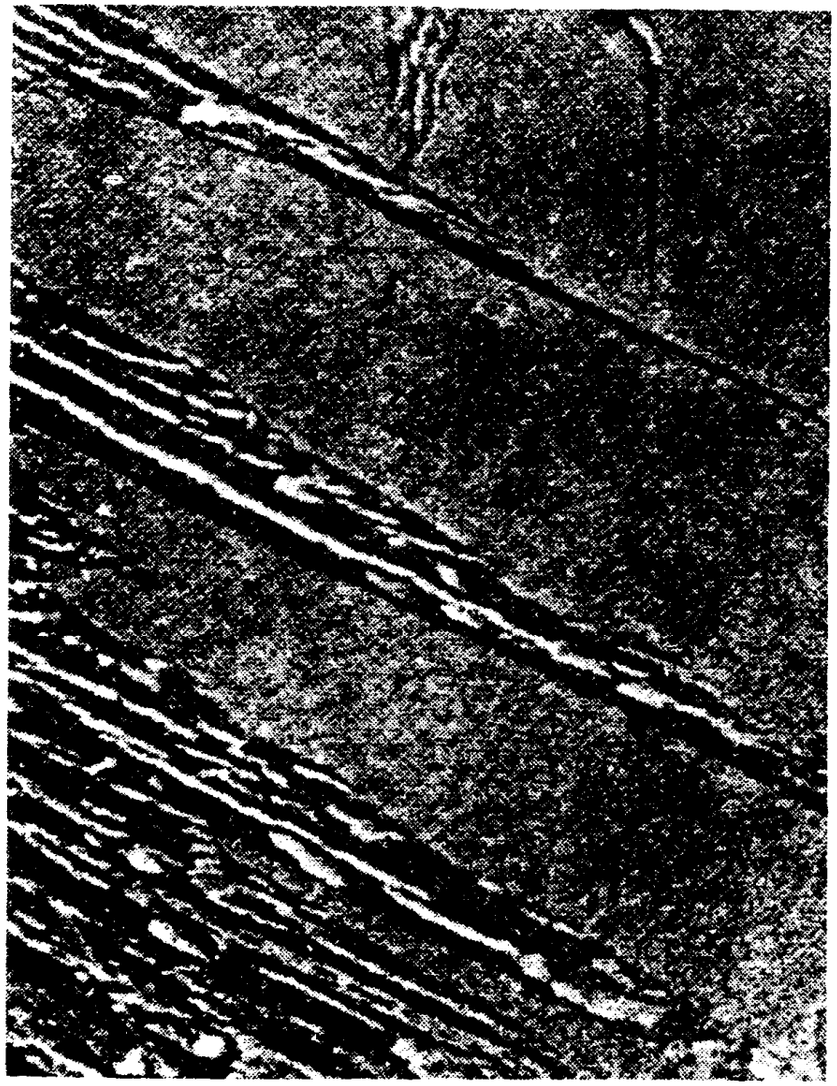

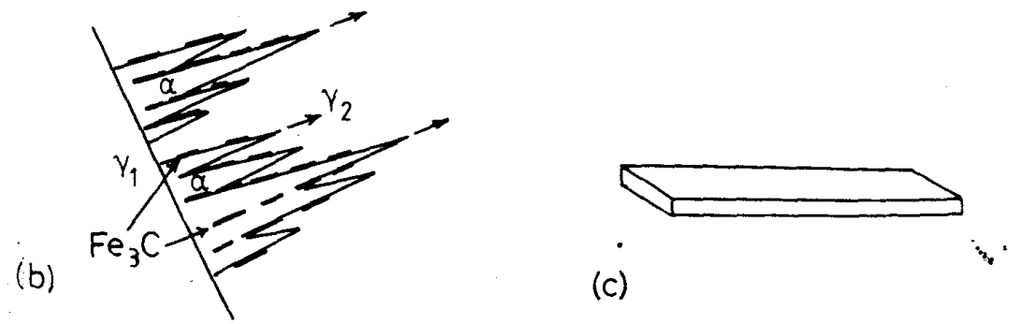

Fig. 5.61 (a) Upper bainite in medium-carbon steel (replica × 13 000) (by permission of the Metals Society). (b) Schematic of growth mechanism. Widmanstätten ferrite laths growth into γ_2. (α and γ_2 have Kurdjumov–Sachs orientation relationship.) Cementite plates nucleate in carbon-enriched austenite. (c) Illustrating the shape of a 'lath'.

faces. This takes place at several sites along the boundary so that a group of finely spaced laths develops. As the laths thicken the carbon content of the austenite increases and finally reaches such a level that cementite nucleates and grows.

At the higher temperatures of formation upper bainite closely resembles finely spaced Widmanstätten side-plates, Fig. 5.46d. As the temperature decreases the bainitic laths become narrower so that individual laths may only be resolved by electron microscopy.

At the highest temperatures where pearlite and bainite grow competitively in the same specimen it can be difficult to distinguish the pearlite colonies from the upper bainite. Both appear as alternate layers of cementite in ferrite. The discontinuous nature of the bainitic carbides does not reveal the difference since pearlitic cementite can also appear as broken lamellae. However, the two microstructures have formed in quite different ways. The greatest difference between the two constituents lies in their crystallography. In the case of pearlite the cementite and ferrite have no specific orientation relationship to the austenite grain in which they are growing, whereas the cementite and ferrite in bainite do have an orientation relationship with the grain in which they are growing. This point is illustrated in Fig. 5.62. The micrograph is from a hypoeutectoid steel (0.6% C) which has been partially transformed at 710 °C and then quenched to room temperature, whereupon the untransformed austenite was converted into martensite. The quench, however, was not fast enough to prevent further transformation at the γ/α interface. The dark constituent is very fine pearlite which was nucleated on the *incoherent* α/γ interface, across which there is no orientation relationship. The ferrite and lower austenite grain, however, have an orientation relationship which has led to bainite formation.

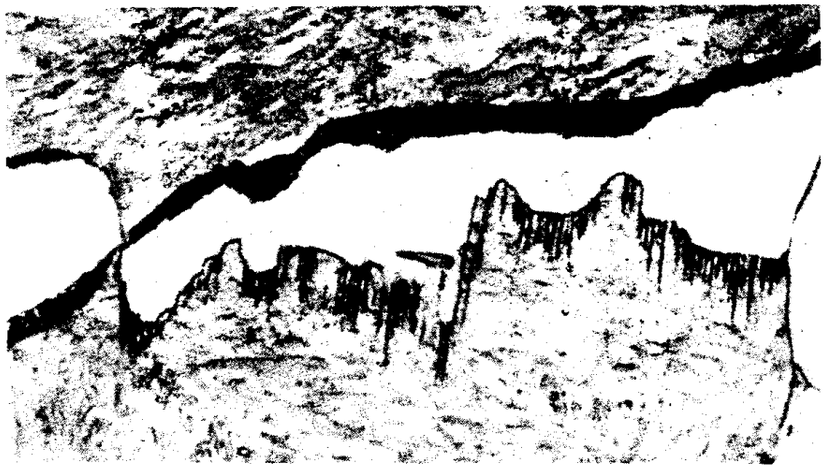

Fig. 5.62 Hypoeutectoid steel (0.6% C) partially transformed for 30 min at 710 °C, inefficiently quenched. Bainitic growth into lower grain of austenite and pearlitic growth into upper grain during quench (× 1800). (After M. Hillert in *Decomposition of Austenite by Diffusional Processes*, V.F. Zackay and H.I. Aaronson (Eds.), 1962, by permission of the Metallurgical Society of AIME.)

Lower Bainite

At sufficiently low temperatures the microstructure of bainite changes from laths into plates and the carbide dispersion becomes much finer, rather like in tempered martensite. The temperature at which the transition to lower bainite occurs depends on the carbon content in a complex manner. For carbon levels below about 0.5wt% the transition temperature increases with increasing carbon, from 0.5–0.7wt% C it decreases and above approximately 0.7wt% C it is constant at about 350 °C. At the temperatures where lower bainite forms the diffusion of carbon is slow, especially in the austenite and carbides precipitate in the ferrite with an orientation relationship. The carbides are either cementite or metastable transition carbides such as ε-carbide and they are an aligned at approximately the same angle to the plane of the ferrite plate (Fig. 5.63). The habit plane of the ferrite plates in lower bainite is the same as that of the martensite that forms at lower temperatures in the same alloy. As with upper bainite, some carbides can also be found between the ferrite plates.

The different modes of formation of upper and lower bainite result in different transformation kinetics and separate C curves on the TTT diagram. An example, the case of a low-alloy steel, is shown in Fig. 5.68.

Transformation Shears

If a polished specimen of austenite is transformed to bainite (upper or lower) it is found that the growth of bainite laths or plates produces a surface relief effect like that of martensite plates. For example Fig. 5.64 shows the surface tilts that result from the growth of lower bainite plates. This has been interpreted as suggesting that the bainite plates form by a shear mechanism in the same way as the growth of martensite plates (see Chapter 6). In other words it is supposed that the iron atoms are transferred across the ferrite/austenite interface in an ordered military manner. However, the growth rate of the bainite plates is controlled by the rate at which carbon can diffuse away from the interface, or by the rate at which carbides can precipitate behind the interface, whereas martensite plates are able to advance without any carbon diffusion, and the plates can grow as fast as the glissile interfaces can advance.

There is, however, much uncertainty regarding the mechanism by which bainitic ferrite grows, and the nature of the austenite–ferrite interface in martensite and bainite. In fact the formation of Widmanstätten side-plates also leads to surface tilts of the type produced by a shear transformation. Also the phenomenological theory of martensite is able to account for the observed orientation relationships and habit planes found in Widmanstätten plates as well as bainite and martensite. It can be seen, therefore, that some phase transformations are not exclusively military or civilian, but show characteristics common to both types of transformation. For a detailed review of the bainite transformation the reader should consult the article by Bhadeshia and Christian, given in the Further Reading section at the end of this chapter.

5.8.3 The Effect of Alloying Elements on Hardenability

The primary aim of adding alloying elements to steels is to increase the hardenability, that is, to delay the time required for the decomposition into

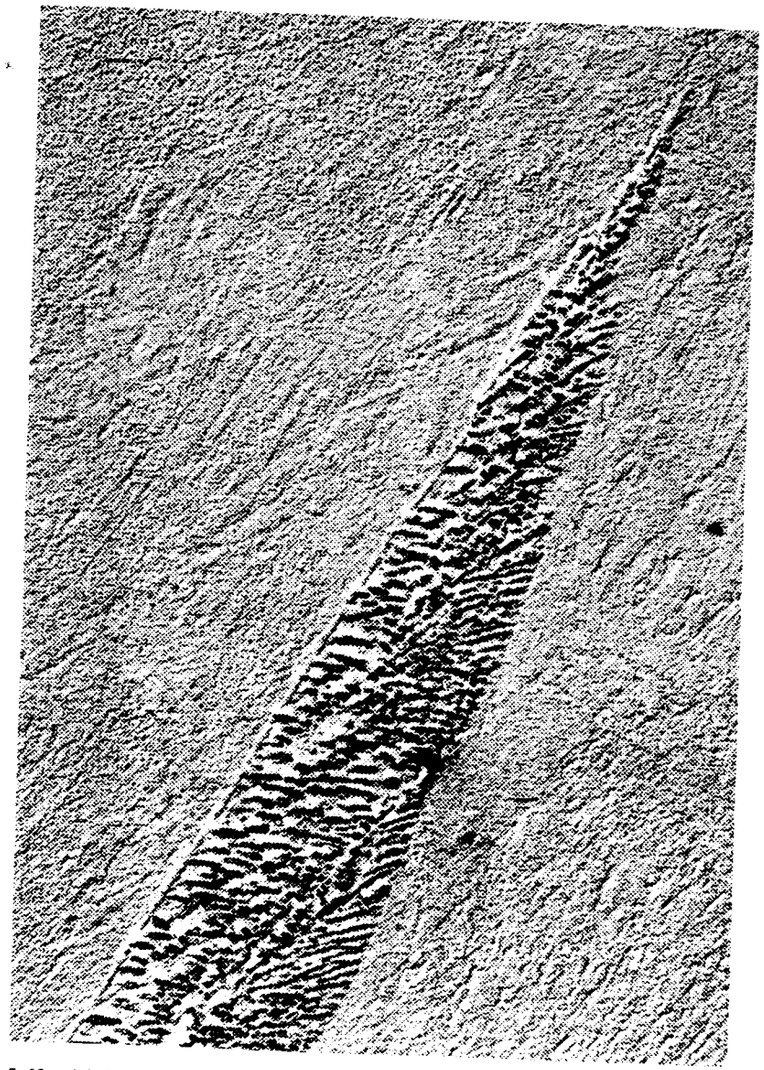

Fig. 5.63 (a) Lower bainite in 0.69wt% C low-alloy steel (replica × 1100). (After R.F. Heheman in *Metals Handbook*, 8th edn., Vol. 8, American Society for Metals, 1973, p. 196.) (b) A possible growth mechanism. α/γ interface advances as fast as carbides precipitate at interface thereby removing the excess carbon in front of the α.

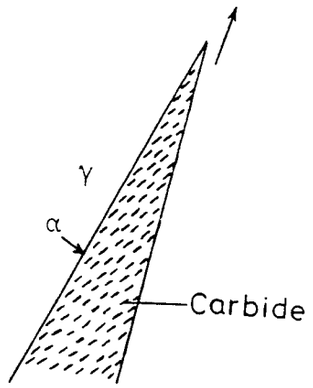

(b)

Fig. 5.63 (*continued*)

ferrite and pearlite. This allows slower cooling rates to produce fully martensitic structures. Figure 5.65 shows some examples of TTT diagrams for various low-alloy steels containing Mn, Cr, Mo and Ni in various combinations and concentrations. Note the appearance of two separate C curves for pearlite and bainite, and the increasing time for transformation as the alloy content increases.

Basically there are two ways in which alloying elements can reduce the rate of austenite decomposition. They can reduce either the growth rate or the nucleation rate of ferrite, pearlite, or bainite.

The main factor limiting hardenability is the rate of formation of pearlite at the nose of the C curve in the TTT diagram. To discuss the effects of alloy elements on pearlite growth it is necessary to distinguish between austenite stabilizers (e.g. Mn, Ni, Cu) and ferrite stabilizers (e.g. Cr, Mo, Si). Austenite stabilizers depress the A_1 temperature, while ferrite stabilizers have the opposite effect. All of these elements are substitutionally dissolved in the austenite and ferrite.

At equilibrium an alloy element X will have different concentrations in cementite and ferrite, i.e. it will partition between the two phases. Carbide-forming elements such as Cr, Mo, Mn will concentrate in the carbide while elements like Si will concentrate in the ferrite. When pearlite forms close to the A_1 temperature the driving force for growth will only be positive if the equilibrium partitioning occurs. Since X will be homogeneously distributed within the austenite, the pearlite will only be able to grow as fast as *substitutional* diffusion of X allows partitioning to occur. The most likely diffusion route for substitutional elements is through the γ/α and γ/cementite interfaces. However, it will be much slower than the interstitial diffusion of carbon and will therefore reduce the pearlite growth rate.